Applied Catalysis B: Environmental 165 (2015) 642–650

Contents lists available at ScienceDirect

Applied Catalysis B: Environmental

journal homepage: www.elsevier.com/locate/apcatb

Full Length Article

Synthesis of glycerol carbonate from the transesterification of dimethyl carbonate with glycerol using DABCO and DABCO-anchored Merrifield resin

Fidelis Stefanus Hubertson Simanjuntak[a,1], Ji Sik Choi[a,1], Gunuk Lee[b], Hye Jeong Lee[b], Sang Deuk Lee[a], Minserk Cheong[b], Hoon Sik Kim[b,*], Hyunjoo Lee[a,**]

[a] Clean Energy Research Center, Korea Institute of Science and Technology, 39-1 Hawolgok-dong, Sungbuk-gu, Seoul 136-791, Republic of Korea
[b] Department of Chemistry and Basic Research Institute of Science, Kyung Hee University, 1 Hoegi-dong, Dongdamun-gu, Seoul, Republic of Korea

ARTICLE INFO

Article history:
Received 25 August 2014
Received in revised form 21 October 2014
Accepted 27 October 2014
Available online 1 November 2014

Keywords:
Glycerol
Dimethyl carbonate
Glycerol carbonate
Immobilization
DABCO

ABSTRACT

Both DABCO (1,4-diazabicyclo[2.2.2]octane) and Merrifield resin-anchored DABCO ([*p*-DABCO]Cl), prepared from the reaction of DABCO and Merrifield resin, were found to exhibit high activities for the transesterification of dimethyl carbonate (DMC) with glycerol to produce glycerol carbonate (GLC). FT-IR and NMR spectroscopic results suggest that such a high transesterification activity of DABCO could be attributed to its superior ability to activate glycerol via a strong hydrogen bond formation between a hydroxyl group of glycerol and an amino group of DABCO. Meanwhile, the activation of glycerol by [*p*-DABCO]Cl proceeds mainly through the hydrogen bond interaction between a hydroxyl group or groups of glycerol and Cl^- of [*p*-DABCO]Cl. The catalytic activity of [*p*-DABCO]Cl was maintained up to 5 reuses, demonstrating that [*p*-DABCO]Cl could be used as a recyclable heterogeneous catalyst.

1. Introduction

Glycerol carbonate (GLC) is a 5-membered cyclic compound having two reactive functional groups: carbonate and hydroxyl groups. For this reason, GLC can be used in many application areas: as a monomer of one- or multi-component polyurethanes, a solvent in the cosmetics industry, a membrane component for gas separation, and a component of coatings and detergents [1–5]. Much effort has been devoted to develop economically viable synthetic processes to prepare GLC from glycerol and various carboxylation sources, including CO_2, urea, and dialkyl carbonates. Among these, the direct carboxylation of glycerol by CO_2 could be considered the most attractive and environmentally benign pathway leading to GLC because the process uses CO_2, a global warming gas, as a raw material, and water is the only byproduct. Accordingly, a number of homogeneous and heterogeneous catalysts such as zeolites, CeO_2/Al_2O_3, and Sn-based compounds have been developed for the carboxylation of glycerol [6–9]. However, the result has never been satisfactory in terms of GLC yield and selectivity. As an alternative to CO_2, urea has been extensively investigated using zirconium phosphate, zinc compounds and hydrotalcite as catalysts [10–12]. Although the urea process is highly efficient for the production of GLC, the reaction must be conducted at elevated temperature under vacuum to remove NH_3 to shift the equilibrium towards the formation of GLC. The synthesis of GLC via transesterification of dimethyl carbonate (DMC) with glycerol under mild condition has also been reported (Scheme 1). A number of base catalysts including KOH, NaOH, K_2CO_3, CaO, $Ca(OH)_2$, and $CaCO_3$ were proven to be highly active for the transesterification, producing GLC in high yield and selectivity [13–16]. Recently, cyclic diamines such as, 1,8-diazabicyclo [5.4.0] undec-7-ene (DBU) and 1,4-diazabicyclo[2.2.2]octane (DABCO) were also found to exhibit high catalytic activities for the transesterification of glycerol with DMC [17,18]. Nevertheless, the use of those alkali, alkaline earth metal and amine compounds as catalysts possesses a drawback in terms of catalyst recovery and reuse because they are inherently homogeneous or tend to transform into homogeneous species with progress of the transesterification. Moreover, the separation of high boiling GLC and glycerol from the transesterification reaction mixtures by distillation in the presence of homogeneous catalysts at elevated temperatures often results in the severe decomposition of the product, GLC along with the formation of side products.

* Corresponding author. Tel.: +82 2 958 5868; fax: +82 2 958 5809.
** Corresponding author.
E-mail addresses: khs2004@khu.ac.kr, hoonsik2@gmail.com (H.S. Kim), hjlee@kist.re.kr (H. Lee).
[1] These authors equally contributed.

http://dx.doi.org/10.1016/j.apcatb.2014.10.071
0926-3373/

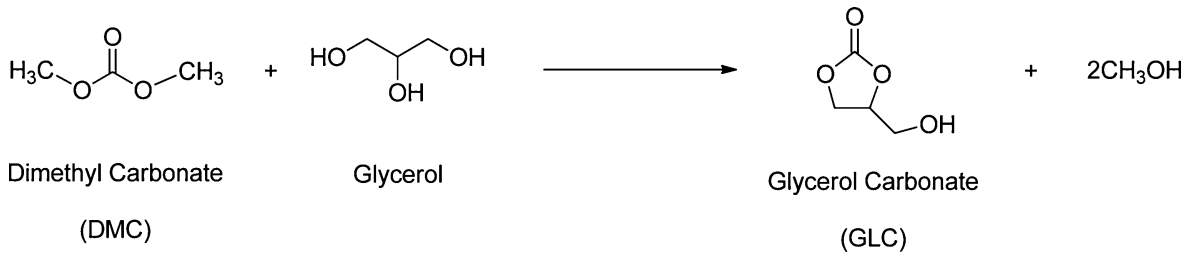

Scheme 1. Synthesis of glycerol carbonate (GLC) from glycerol and dimethyl carbonate (DMC).

For facile catalyst recovery, heterogeneous base catalysts such as Mg-Al hydrotalcite, Mg–La mixed oxide, Mg/Al/Zr, and $Mg_{1.2}Ca_{0.8}O_2$ mixed oxides were tested for their activities toward the transesterification. High yields of GLC were attained with those catalysts, but only with considerably large amounts of catalyst loadings [19–24].

With these considerations in mind, we have attempted to develop heterogeneous catalysts that are easy to prepare, cost-effective, and free of leaching. To this end, we first focused on the immobilization of a polyamine onto polymeric materials. Polyamines are organic bases having two or more amine functional groups in a molecule. It was expected that one of the amine functional groups of an immobilized polyamine could be used as a linker to the solid surface, and the remaining amine functional group or groups could act as active sites to catalyze the transesterification reaction.

Herein, we report on the synthesis of several Merrifield peptide resin-anchored polyamines and their use as heterogeneous catalysts for the transesterification of DMC with glycerol.

2. Experimental

2.1. Materials

Merrifield peptide resin (Cl content: 2.4 mmol/g) was obtained from Tokyo Chemical Industry. Solvents, DMC, glycerol, GLC, and polyamines, including 1,4-diazabicyclo[2.2.2]octane (DABCO), *N*,*N*,*N*′,*N*′-tetramethylethane-1,2-diamine (TMEDA), *N*,*N*,*N*′,*N*″,*N*″-pentamethyldiethylene triamine (PMDTA), and 4-(dimethylamino)pyridine (DMAP) were purchased from Sigma Aldrich Chemical Co. All reagents were used as received without further purifications.

2.2. Instrumentation

Solid state ^{13}C NMR spectra were recorded on a Bruker Avance 400 WB equipped with a CP-MAS (cross polarization magic-angle-spinning) accessory. FT-IR spectra of catalyst samples were recorded on a Nicolet FT-IR spectrometer (iS10, USA) equipped with a SMART MIRACLE accessory. The elemental analysis of the fresh and spent immobilized catalysts was conducted on a Thermo Elemental Analyzer Scientific Flash 2000 (Thermo Scientific USA). The pKa values of polyamines and benzylated polyamines were measured using an automatic potentiometric titrator (AT-700, KEM, Japan).

2.3. Immobilization of polyamines onto Merrifield resin

In a typical synthesis, Merrifield peptide resin (2 g) in acetone (25 ml) was refluxed with DABCO (10 mmol) for 24 h with a gentle stirring. At the end of the reaction, the resulting DABCO-immobilized resin was filtered, washed with fresh acetone and diethyl ether to remove excess DABCO, and finally dried under a vacuum for 8 h. Elemental analysis: C 76.4%, H 8.6%, N 5.3%.

TMEDA-immobilized Merrifield resin was prepared in a similar manner to that employed in the synthesis DABCO-immobilized Merrifield resin. Elemental analysis: C 73.9%, H 8.9%, N 5.3%.

2.4. Transesterification of DMC with glycerol

In a typical reaction, glycerol (108.5 mmol), dimethylcarbonate (DMC, 217.0 mmol) and a polyamine or a polyamine-immobilized Merrifield resin catalyst were loaded into a 100 mL round-bottom flask equipped with a reflux condenser. The flask was then heated to a desired temperature with stirring using an electrical heater. After the completion of the reaction, the flask was cooled to room temperature, and the product mixture was analyzed using a HPLC (Waters) equipped with an Aminex HPX-87H column (Biorad) and a RI detector (Waters 410). The mobile phase used was a 5 mM H_2SO_4 aqueous solution, and the flow rate was set at 0.6 mL/min.

2.5. Quantum mechanical calculation

The interaction of glycerol with [methyl-DABCO]Cl ([MDABCO]Cl) and [methyl-TMEDA]Cl ([MTMEDA]Cl) were theoretically investigated using a Gaussian 03 program [25]. For simplicity, [MDABCO]Cl and [MTMEDA]Cl were chosen as the model compounds of [*p*-DABCO]Cl and [*p*-TMEDA]Cl, respectively. The geometry optimizations and thermodynamic corrections were performed with hybrid Becke 3-Lee–Yang–Parr (B3LYP) exchange–correlation functional with the 6-31 + G* basis sets for C, H, N, O, and Cl. In order to obtain the most stable geometries, all kinds of possible interaction patterns were optimized. No restrictions on symmetries were imposed on the initial structures. All stationary points were verified as minima by full calculation of the Hessian and a harmonic frequency analysis.

3. Results and discussions

3.1. Polyamine-catalyzed transesterification of DMC with glycerol

Four different polyamines, including DABCO ($pK_b = 5.2$; $pK_a = 8.8$), TMEDA ($pK_b = 5.0$; $pK_a = 11.0$), PMDTA ($pK_b = 4.9$; $pK_a = 9.1$), and DMAP ($pK_b = 4.3$; $pK_a = 5.2$), were evaluated for their activities for the transesterification of DMC with glycerol [26–28]. The structures of the polyamines tested in this study were depicted in Fig. 1.

3.1.1. Activities of polyamines

Carbomethoxylation reaction of glycerol with DMC was conducted at 80 °C with the molar ratios of DMC/glycerol and glycerol/catalyst at 2 and 1000, respectively, and the amount of glycerol was fixed at 10 g (108.5 mmol). Samples were withdrawn every 10 min and analyzed by HPLC. As can be seen in Fig. 2, DABCO afforded much higher GLC yield than the other three amines tested. For the DABCO-catalyzed reaction, GLC was produced in yield of 4.7% in the early stage of the reaction at 10 min, whereas

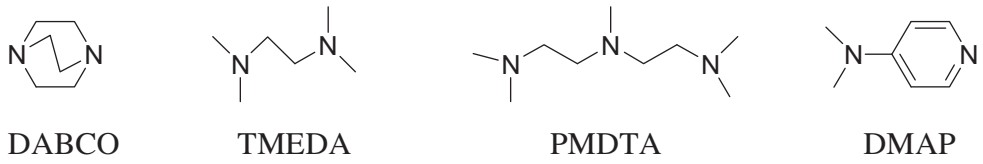

Fig. 1. Structures of polyamines used as catalysts for the transesterification of glycerol with DMC.

the yield of GLC in the presence of other polyamines was negligible up to 20 min. After 1 h of the reaction, the yields of GLC were 54.8, 21.0, 23.8, and 6.2% for DABCO, TMEDA, PMDTA, and DMAP-catalyzed reactions, respectively. Considering that the first pK_b value of DABCO is almost same as those of other three polyamines, approximately more than two times higher activity of DABCO compared with those of other amines is difficult to explain by the amine basicity alone. DABCO has a rigid and compact cage-like structure, and thus the lone pairs on the nitrogen atoms are not disturbed by the neighboring alkylene groups [29]. For this reason, DABCO seems to exhibit much stronger nucleophilicity than other polyamines with similar basicities. As a result, DABCO is capable of forming stronger hydrogen bonds with glycerol via nitrogen atom or atoms than other polyamines, thereby facilitating the nucleophilic attack of glycerol on the carbonyl carbon of DMC. In view of this, the higher activity of DABCO can be ascribed to the higher nucleophilicity of DABCO. It was expected that PMDTA with three amino groups would exhibit higher activity than TMEDA with two amino functionalities. However, comparison of the GLC yields suggests that the catalytic activity is not closely related to the number of amine functional groups in the molecule.

3.1.2. *FT-IR study on the interactions of glycerol with polyamines*

To gain insight into the reaction mechanism of the transesterification catalyzed by polyamines, the interactions of glycerol and DMC with DABCO or TMEDA were investigated by FT-IR spectroscopy. As can be seen in Fig. 3, upon interaction of glycerol with DABCO in a molar ratio of 2:1, the broad absorption peak centered at 3291 cm^{-1} associated with the O—H stretching frequency of glycerol was found to split into two peaks at 3362 and 3130 cm^{-1}. This strongly suggests that there are two types of O—H groups toward the interaction with DABCO. The peak at lower frequency of 3130 cm^{-1} can be assigned to the hydroxyl group or groups of glycerol interacting with a nitrogen atom of DABCO via hydrogen bond or bonds. In consideration of the large degree of peak shift to a lower frequency by approximately 160 cm^{-1}, it is obvious that the bond strength of O—H group or groups interacting with DABCO is greatly reduced by the strong hydrogen bond interaction. The peak appeared at a higher frequency of 3362 cm^{-1} could be associated with the O—H groups of glycerol, which are not involved in the hydrogen bond interaction with DABCO. This is reasonable because the increase of the O—H bond length of a hydroxyl group or groups caused by hydrogen bonding will obviously result in the shortening of the O—H bond length of the remaining hydroxyl groups.

Similar behavior was also observed for the interaction of TMEDA with glycerol, two absorption bands assignable to the O—H stretching frequencies appeared at 3385 and 3206 cm^{-1}. It is worth to note that the degree of peak shift to a lower frequency is 85 cm^{-1}, which is smaller by 76 cm^{-1} compared with that observed for the interaction with DABCO. As deduced from the result of transesterification activity test, the degree of O—H peak shift for the interactions of glycerol with PMDTA was very close to that observed for the interaction of glycerol with TMEDA (see Fig. S1 in Supporting Information). On the contrary, the O—H peak shift was almost negligible for the interaction of DMAP with glycerol. This implies that the availability nonbonding electron pairs on the nitrogen atoms of DMAP toward the hydrogen bonding interaction with glycerol are extremely restricted due to the methyl groups on the nitrogen atoms. From the correlation of transesterification activity with the degree of O-H peak shift, it is evident that the catalytic activity of a polyamine is largely governed by its hydrogen bonding ability to activate glycerol.

3.2. *Transesterification catalyzed by polyamine-anchored Merrifield resins*

Although the polyamines, especially DABCO, are found to be highly efficient catalysts for the transesterification of DMC with glycerol, there remains one major drawback to overcome in terms of catalyst recovery. Facile recovery and reuse of a catalyst from a

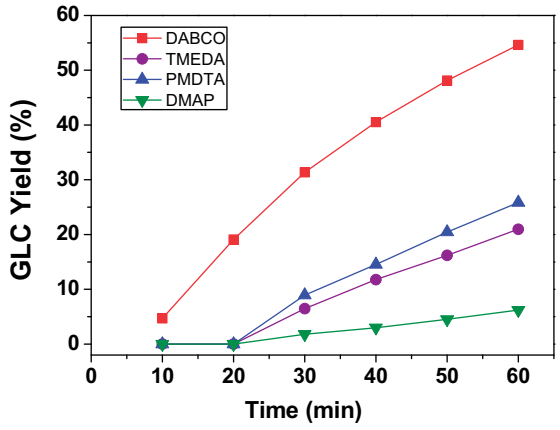

Fig. 2. Polyamine-catalyzed transesterification of DMC by glycerol with time. Reaction condition: glycerol = 10 g, molar ratio of DMC/glycerol = 2, molar ratio of glycerol/catalyst = 1000, T = 80 °C.

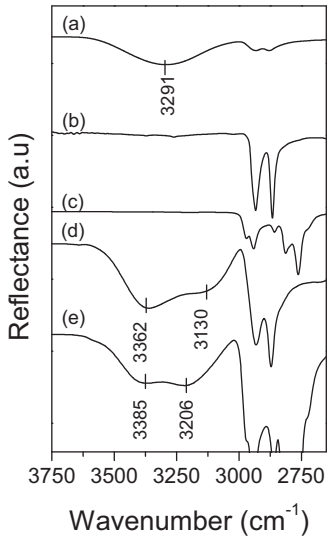

Fig. 3. FT-IR spectra of (a) glycerol, (b) DABCO, (c) TMEDA, (d) glycerol + DABCO (molar ratio: 2/1), and (e) glycerol + TMEDA (molar ratio: 2/1).

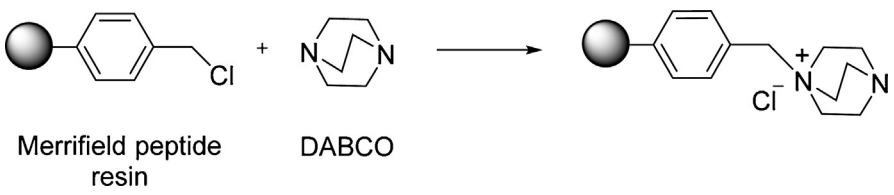

Scheme 2. Synthesis of DABCO-anchored Merrifield resin ([*p*-DABCO]Cl).

reaction mixture are very important in the evaluation of economic feasibility of a catalytic process.

For this reason, we have attempted to heterogenize polyamines through immobilization onto a polymer support. To this end, Merrifield resin has been chosen because it is a chloromethylated polystyrene-based resin, from which the covalently bound chlorine atoms can be easily replaced by tertiary amines. A number of reports have already been disclosed on the immobilization of DABCO onto solid supports, such as silica and polystyrene as well as on the application of immobilized DABCO as catalysts for several reactions, including asymmetric aldol condensation, Knoevenagel condensation, and synthesis of 4*H*-benzo[*b*]pyran derivatives [30–32]. However, the immobilization of polyamines onto Merrifield resin and their application as catalysts for the synthesis of GLC have rarely been investigated. As DABCO was shown to exhibit more than two times higher activity than the other polyamines tested, the immobilization was conducted only with DABCO and TMEDA.

3.2.1. Synthesis of polyamine-anchored Merrifield resin, [p-polyamines]Cl

Merrifield resin-supported polyamines were prepared by reacting Merrifield resin with a corresponding polyamine in acetone at reflux for 24 h. The immobilization of a polyamine on Merrifield resin is depicted in Scheme 2 using DABCO as the representative polyamine. Elemental analysis of the resulting polyamine-anchored Merrifield resins revealed that all of the covalently bound chlorine atoms in the Merrifield resin were completely substituted by DABCO or TMEDA, resulting in the formation of [*p*-DABCO]Cl and [*p*-TMEDA]Cl (see Table S1 in Supporting Information).

The basicity of [*p*-DABCO]Cl and [*p*-TMEDA]Cl could be estimated from the basicity of benzyl substituted ones, [*bz*-DABCO]Cl and [*bz*-TMEDA]Cl, which could be obtained by using titration method and NMR measurements [33]. It is worth to note that the basicity of [*bz*-DABCO]Cl ($pK_b = 11.8$; $pK_a = 5.2$) is much lower than that of [*bz*-TMEDA]Cl ($pK_b = 8.2$; $pK_a = 5.8$) although the parent diamines, TMEDA and DABCO possess similar pK_b values of 5.0 and 5.2, respectively. Such a drastic change in basicity after the quaternization of one of the amino groups of diamines could be ascribed to the difference in the degree of charge delocalization between the positively charged and the neutral nitrogen atoms via a bridging ethylene group or groups. It is likely that charge transfer between quaternized and unquaternized nitrogen atoms takes place more easily as the number of bridging ethylene groups connecting two nitrogen atoms increases. In view of this, the weaker basicity of [*p*-DABCO]Cl with three bridging ethylene groups compared with that of [*p*-TMEDA]Cl with one bridging ethylene group could be rationalized.

3.2.2. Spectroscopic characterization of polyamine-anchored Merrifield resins, [p-polyamine]Cl

Polyamine-anchored Merrifield resins, [*p*-DABCO]Cl and [*p*-TMEDA]Cl were characterized by ^{13}C-Mas NMR spectroscopy. As can be seen in Fig. 4, comparison of the ^{13}C-Mas NMR spectra of DABCO, Merrifield resin, and [*p*-DABCO]Cl shows that the chemical shifts of the methylene groups of DABCO and Merrifield resin moved downfield to a great extent from 47.3 and 46.0 ppm to 52.6 and 66.0 ppm, respectively. This clearly demonstrates that DABCO was successfully immobilized onto Merrifield resin. The new peaks appeared at 66.0 and 52.6 ppm in the NMR spectrum of [*p*-DABCO]Cl can be assigned to benzylic CH_2—N^+ of Merrifield resin and CH_2—N^+ of DABCO, respectively. The peak at 46.1 ppm was assigned to the methylene groups bonded to the unquaternized nitrogen atom of the immobilized DABCO. Any sign of double quaterizations on the nitrogen atoms of DABCO by Merrifield resin was not observed. Likewise, new peaks appeared at 64.8 and 51.7 ppm at the resin anchored TMEDA could be associated with the methylene and methyl group bonded to quaternized nitrogen atom in [*p*-TMEDA]Cl, respectively.

The immobilization of polyamines onto the Merrifield resin was further supported by FT-IR spectroscopy (Fig. S2 in Supporting Information). The C—Cl stretching frequency at 1260 cm^{-1}, a characteristic peak of Merrifield resin, was no longer observed in the FT-IR spectra of [*p*-DABCO]Cl and [*p*-TMEDA]Cl, indicating that Merrifield resin was completely converted into [*p*-DABCO]Cl and [*p*-TMEDA]Cl. The appearance of new peaks at 1052 cm^{-1} and 1034 cm^{-1} assignable to C—N stretching frequency is strong evidence that DABCO and TMEDA were immobilized onto Merrifield resin [32,34].

3.2.3. Activity of polyamine-anchored Merrifield resin

Transesterification of DMC with glycerol was conducted at 80 °C for 1 h using [*p*-DABCO]Cl or [*p*-TMEDA]Cl as the catalyst. The molar ratio of glycerol/diamine in the resin catalyst was fixed at 100. As listed in Table 1, the GLC yield obtained in the presence of [*p*-DABCO]Cl was more than 5.5 times of that with [*p*-TMEDA]Cl (68.4% vs. 11.7%). This is rather an unexpected result because the basicity of [*p*-TMEDA]Cl ($pK_b = 8.2$; $pK_a = 5.8$) is much stronger than that of [*p*-DABCO]Cl ($pK_b = 11.8$; $pK_a = 2.2$). This result may imply that the catalytic performance of a polyamine-anchored resin catalyst toward the transesterification is not solely dependent

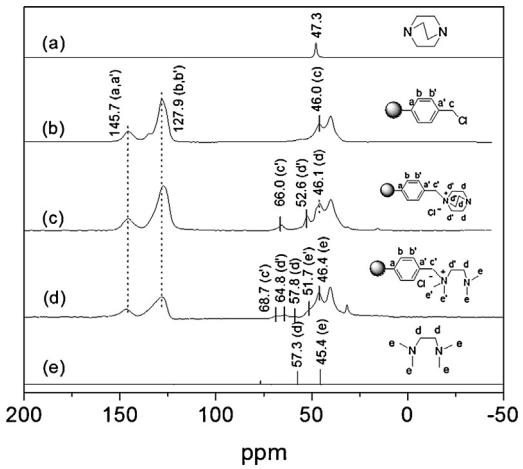

Fig. 4. ^{13}C-MAS NMR spectra of (a) DABCO, (b) Merrifield resin, (c) [*p*-DABCO]Cl, (d) [*p*-TMEDA]Cl, and (e) ^{13}C-NMR spectrum of TMEDA in $CDCl_3$.

Table 1
Catalytic activities of diamines and amine-anchored Merrifield resins[a]

Catalyst	*C* (%)	*Y* (%)	*S* (%)	TOF (h^{-1})[b,c]
Merrifield resin	–	–	–	–
TMEDA	21.8	20.9	95.9	209.0
DABCO	56.0	54.6	97.5	546.0
[*p*-TMEDA]Cl	14.1	11.7	83.0	11.7
[*p*-DABCO]Cl	69.8	68.5	98.1	68.5
[*p*-DABCO]CH_3SO_3	42.5	40.8	96.0	40.8
[*p*-DABCO]BF_4	17.0	14.7	86.5	14.7
[*p*-TEA]Cl	15.4	12.4	80.5	12.4

[a] Reaction condition: glycerol = 10 g, molar ratio of DMC/glycerol = 2, molar ratio of glycerol/catalyst = 1,000 for diamines and 100 for resin-anchored amines, $T = 80\,^{\circ}C$, $t = 1$ h. *C*: conversion of glycerol, *Y*: yield of GLC, *S*: selectivity of GLC.
[b] TOF (h^{-1}) for diamines = mol GLC produced/mol diamine/h.
[c] TOF (h^{-1}) for amine-anchored resins = mol GLC produced/mol amine in the resin catalyst/h.

on the basicity of the catalyst. It is suggested that both the unquaternized amino group of cation and the chloride anion could play catalytic roles, possibly in a cooperative mode (*vide infra*).

The participation of anion in the catalysis is somewhat supported by comparing the activity of [*p*-DABCO]Cl with those of [*p*-DABCO] CH_3SO_3 and [*p*-DABCO]BF_4. Table 1 also reveals that the activity of the diamine anchored resin catalyst is strongly affected by the type of anion. When [*p*-DABCO]Cl was replaced by [*p*-DABCO]CH_3SO_3 and [*p*-DABCO]BF_4, GLC yield was found to decrease from 68.5% to 40.8 and 14.7%, respectively. It has been reported that the hydrogen bond basicities of Cl^-, $CH_3SO_3^-$, and BF_4^- are 0.95, 0.85, and 0.36, respectively, for the 1-butyl-3-methylimidazolium-based salts [35,36]. From this result, it is likely that the activity of the diamine anchored resin catalyst is closely related to the anion basicity. In view of this, it is assumed that the cation-anion interaction in [*p*-DABCO]Cl is weaker than that in [*p*-TMEDA]Cl, and thus Cl^- of [*p*-DABCO]Cl has stronger hydrogen bond basicity than that of [*p*-TMEDA]Cl. However, it is premature to conclude that the anion basicity is the sole factor in determining the activity of [*p*-DABCO]Cl without considering the structure and the basicity of the cation because the activity of triethylamine anchored Merrifield resin ([*p*-TEA]Cl) is much lower than that of [*p*-DABCO]Cl (*vide infra*).

It should be mentioned here that the catalytic activities of DABCO and TMEDA were greatly reduced upon immobilization onto Merrifield resin. For instance, as can be seen in Table 1, the turnover frequency (TOF) attained with [*p*-DABCO]Cl was only about 1/8 of that achieved with DABCO. Nonetheless, such a drawback arising from the use of [*p*-DABCO]Cl could be balanced to some extent by easier catalyst recovery.

3.2.4. FT-IR study on the interactions of glycerol with polyamine-anchored Merrifield resins

The interactions of glycerol with [*p*-DABCO]Cl and [*p*-TMEDA]Cl in a 2:1 molar ratio were investigated by FT-IR spectroscopy. However, as can be seen in Fig. S3 (Supporting Information), the O-H peak shift of glycerol was not distinct. This is in great contrast to the interaction of glycerol with DABCO and TMEDA, where the O—H peak of glycerol was split into two peaks. It seems that the hydrogen bonding interaction of glycerol with [*p*-DABCO]Cl or [*p*-TMEDA]Cl is not strong enough to split the O—H peak of glycerol into two, and thus all the absorption bands of O—H peaks of glycerol are overlapped and look apparently unchanged. In order to observe the change in O—H peak shift arising from the hydrogen bonding, [*p*-DABCO]Cl or [*p*-TMEDA]Cl were interacted with 2-methoxyethanol (MEG) with only one hydroxyl group. As shown in Fig. 5, the broad peak centered at 3407 cm^{-1} corresponding to the O—H stretching frequency of MEG was found to shift by 81 and 65 cm^{-1} to lower frequencies at 3326 and 3342 cm^{-1} on interactions

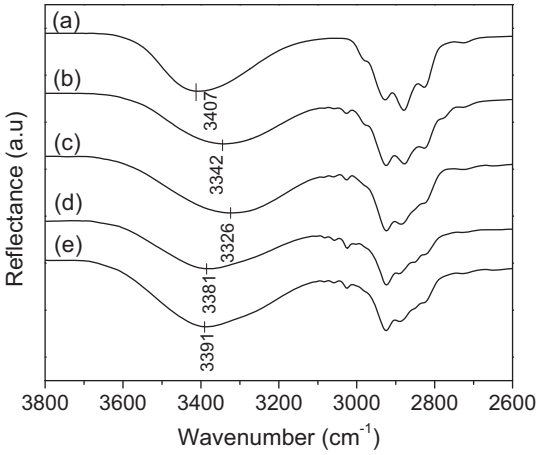

Fig. 5. FT-IR spectra of (a) MEG, (b) MEG + [*p*-TMEDA]Cl (weight ratio: 2/1) and (c) MEG + [*p*-DABCO]Cl (weight ratio: 2/1), (d) MEG + [*p*-DABCO]CH_3SO_3 (weight ratio: 2/1), and (e) MEG + [*p*-DABCO]BF_4 (weight ratio: 2/1).

with [*p*-DABCO]Cl and [*p*-TMEDA]Cl, respectively. Although the degrees of O—H peak shift are much smaller than those observed for the interactions of glycerol with DABCO or TMEDA, it is obvious that the hydroxyl group of MEG interacts with [*p*-DABCO]Cl and [*p*-TMEDA]Cl. The degree of O-H peak shift for the interaction of MEG with [*p*-DABCO]Cl was larger by 16 cm^{-1} than that with [*p*-TMEDA]Cl, suggesting that [*p*-DABCO]Cl is more effective than [*p*-TMEDA]Cl for activating alcohol. This is probably the reason why [*p*-DABCO]Cl affords higher GLC yield than [*p*-TMEDA]Cl.

To more clearly see the effect of hydrogen bonding on the catalytic activity, FT-IR spectroscopic investigation was also conducted for the interactions of MEG with [*p*-DABCO]CH_3SO_3 and [*p*-DABCO]BF_4. As can be seen in Fig. 5, the broad peak centered at 3407 cm^{-1} associated with the O—H stretching frequency of MEG moved by 26 cm^{-1} to lower frequencies at 3381 cm^{-1} on interaction with [*p*-DABCO]CH_3SO_3. In contrast, the O—H peak remained almost unchanged when MEG was mixed with [*p*-DABCO]BF_4. These results again suggest that the activity of a diamine anchored resin is closely related to its hydrogen bonding ability to the hydroxyl group of glycerol.

3.2.5. Computational calculations

To support the experimental and FT-IR spectroscopic results, the interactions of glycerol with [*p*-DABCO]Cl and [*p*-TMEDA]Cl were theoretically investigated. For simplicity, [*p*-DABCO]Cl and [*p*-TMEDA]Cl were replaced by [MDABCO]Cl and [MTMEDA]Cl, respectively. Fig. 6 depicts the optimized structures showing the interaction modes of glycerol with [MDABCO]Cl and [MTMEDA]Cl, respectively. The numbers in parentheses are energies relative to those of the reactants. Two basic sites could be conceivable for the interaction of glycerol with [MDABCO]Cl or [MTMEDA]Cl: unquaternized nitrogen atom and Cl^-. In the optimized structure showing the interaction of glycerol with [MDABCO]Cl, the chloride anion is found to strongly interact with glycerol via two hydroxyl groups (C-1 and C-2 OH). This is reasonable because Cl^- is known to possess a strong hydrogen bond basicity [37]. The remaining terminal hydroxyl group (C-3 OH) is also found to interact with the oxygen atom of the hydroxyl group at C-1 carbon atom. The direct interaction of glycerol with the unquaternized nitrogen atom is not observed, possibly due to the structural rigidity of [MDABCO] cation. The enthalpy (ΔH) for the interaction of [MDABCO]Cl with glycerol ([MDABCO]Cl-glycerol) via Cl^- was calculated as −17.1 kcal/mol. This suggests that the activation of glycerol by [MDABCO]Cl proceeds mainly through the hydrogen bond interactions with Cl^-. The nonbonding electrons on the unquaternized

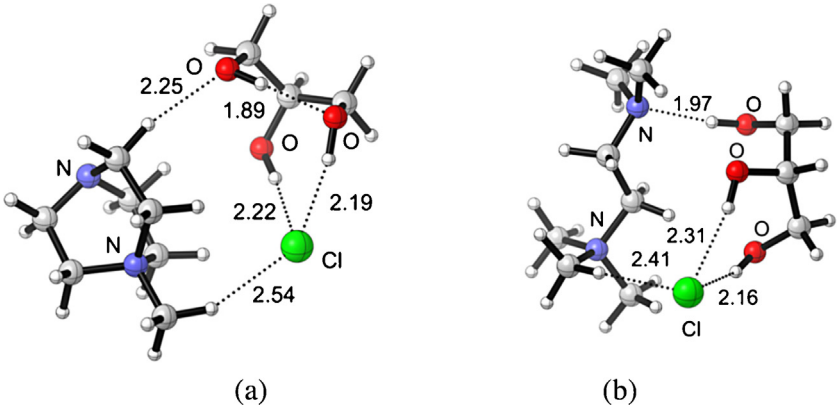

Fig. 6. Optimized structures showing the interaction modes of glycerol with [MDABCO]Cl and [MTMEDA]Cl: (a) with [MDABCO]Cl via Cl^- ($\Delta H = -17.1$ kcal/mol) and (b) with [MTMEDA]Cl via both N and Cl^- ($\Delta H = -9.6$ kcal/mol).

atom remained intact could be available for the interaction with DMC. On the contrary, as shown in Fig. 6(b), in the optimized structure showing the interaction of [MTMEDA]Cl with glycerol, [MTMEDA]Cl-glycerol is found to interact with all three hydroxyl groups of glycerol via both the unquaternized nitrogen atom and Cl^-: one with the unquaternized nitrogen atom and the other two with Cl^-. This is the most striking difference from that observed in the optimized structure of [MDABCO]Cl-glycerol, where glycerol interacts with Cl^- via two hydroxyl groups only. The interaction enthalpy (ΔH) for the optimized structure of [MTMEDA]Cl-glycerol is calculated as −9.6 kcal/mol, which is higher by 7.5 kcal/mol than that of [MDABCO]Cl-glycerol. The nonbonding electrons on the unquaternized nitrogen atom of [MTMEDA]Cl seems to be no longer available toward the interaction with DMC. The lack of available interaction site for DMC and the lower interaction enthalpy could be the reasons for the considerably lower activity of [MTMEDA]Cl compared with that of [MDABCO]Cl.

Although the reaction pathway for the transesterification has not been fully elucidated yet by computational calculation, the optimized structure for the interaction of [MDABCO]Cl-glycerol with DMC ([MDABCO]Cl-glycerol-DMC) shown in Fig. 7(a) demonstrates that DMC is capable of interacting with both the unquaternized nitrogen atom of [MDABCO]Cl and the hydroxyl group of glycerol in a cooperative manner. It is worth to note that the hydrogen bond formed between the C-1 and C-3 hydroxyl groups in the optimized structure of [MDABCO]Cl-glycerol (Fig. 6(a)) is broken and a new hydrogen bond is formed between the C-3 OH and the carbonyl oxygen of DMC in the optimized structure of [MDABCO]Cl-glycerol-DMC (Fig. 7(a)). The calculated interaction enthalpy of [MDABCO]Cl-glycerol-DMC is −0.8 kcal/mole with respect to that of the optimized structure of [MDABCO]Cl-glycerol shown in Fig. 6(a). Fig. 7(b) is the optimized structure of a transition state showing the nucleophilic attack of glycerol on the carbonyl carbon of activated DMC via the oxygen atom of the hydroxyl group at C-3. The chloride anion plays a role as a proton acceptor from the hydroxyl group, thereby enhancing the nucleophilicity of the C-3 hydroxyl oxygen atom.

The optimized structure of the product shown in Fig. 7(c) suggests that the liberation of methanol from the intermediate species and the subsequent formation of GLC might proceed with the aid of Cl^-. The interaction enthalpies for the transition state and the product are calculated as 39.6 and −4.6 kcal/mol, respectively with respect to that of the reactant, [MDABCO]Cl-glycerol-DMC. These calculation results suggest that the [p-DABCO]Cl-catalyzed transesterification could proceed in a cooperative manner, in which both Cl^- and the unquaternized nitrogen atom play catalytic roles.

This is somewhat supported by the different behaviour of [*p*-DABCO]Cl from that of [*p*-TMEDA]Cl toward the interaction with DMC. As can be seen in the FT-IR spectra (Fig. 8), a broad carbonyl peak centered at 1632 cm^{-1} was newly observed when [*p*-DABCO]Cl was interacted with DMC at 50 °C in a 1:2 weight ratio, whereas any peak associated with the interaction between [*p*-TMEDA]Cl and DMC was not seen. The FT-IR spectra shown in Figs. 5 and 8 clearly demonstrate that [*p*-DABCO]Cl is much more reactive toward the interaction with both glycerol and DMC compared with [*p*-TMEDA]Cl.

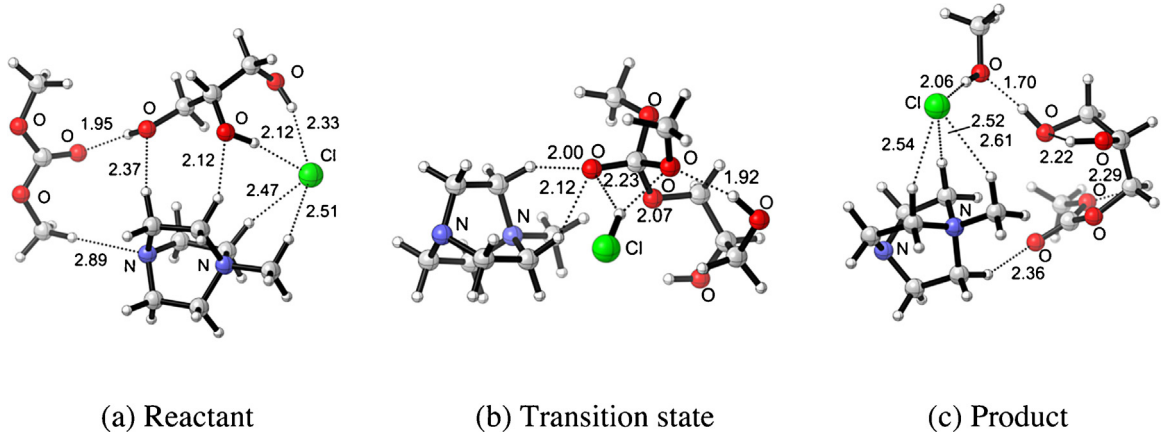

Fig. 7. Optimized structures showing the interaction of [MDABCO]Cl with glycerol with DMC: (a) reactant ($\Delta H = 0$ kcal/mol), (b) Transition state ($\Delta H = +39.6$ kcal/mol), and (c) product ($\Delta H = -4.6$ kcal/mol).

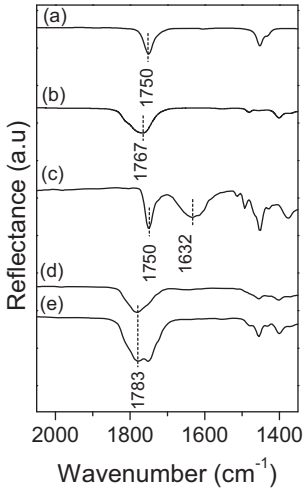

Fig. 8. FT-IR spectra of (a) DMC, (b) GLC (c) [*p*-DABCO]Cl + DMC at 50 °C for 30 min, (d) (c) + glycerol at 80 °C for 30 min, and (e) GLC + DMC (weight ratio: 2/1).

In combination of experimental, spectroscopic, and computational results, it is cautiously concluded that the catalytic activity of a diamine-based salt bearing a chloride anion is strongly affected by its ability to interact with both glycerol and DMC. The chloride anion is mostly responsible for the activation of glycerol, and the unquaternized nitrogen atom contributes to the activation of DMC.

3.3. Proposed mechanism

It has been suggested that the transesterification of DMC with glycerol in the presence of a strong base such as metal hydroxide, metal oxide, or metal carbonate proceeds via a nucleophilic attack of glycerolate anion, generated from the interaction of glycerol with the base, on the carbonyl carbon of DMC [4,13]. However, transesterification in the presence of a weakly basic catalyst such as an ionic liquid seems to proceed in a different manner from that performed in the presence of a strong base, possibly due to the difficulty in generating glycerolate anion from the direct interaction of glycerol with the weak bases. As mentioned earlier, the GLC yield obtained with [*p*-DABCO]Cl is approximately six times higher than that with [*p*-TMEDA]Cl although [*p*-TMEDA]Cl is estimated to exhibit much stronger basicity than [*p*-DABCO]Cl on the basis of the measured pK_b values of [*bz*-TMEDA]Cl and [*bz*-DABCO]Cl having the same structural moieties to [*p*-TMEDA]Cl and [*p*-DABCO]Cl, respectively. This implies that the transesterification reaction is not solely dependent on the basicity of the catalyst. In consideration of this, a plausible mechanism for the [*p*-DABCO]Cl-catalyzed transesterification reaction was suggested on the basis of the experimental, computational, and FT-IR spectroscopic results. As depicted in Scheme 3, the first step is likely to be the activation of glycerol through the hydrogen bonding interaction between the two hydroxyl groups of glycerol and the chloride anion. The second step would be the simultaneous interactions of DMC with the unquaternized nitrogen atom and the remaining hydroxyl group of the activated glycerol, generating intermediate species **II**. The third step is believed to involve the rearrangement of **II** followed by the nucleophilic attack of the activated glycerol on the carbonyl carbon of DMC to generate an intermediate species, **III** with the concomitant loss of methanol. The intramolecular attack of the activated hydroxyl oxygen atom on the carbonyl carbon of **III** and the following cyclization would produce GLC along with the regeneration of the [*p*-DABCO]Cl.

3.4. Effects of reaction conditions

The effect of reaction time on the transesterification of DMC with glycerol was investigated in the range of 30–240 min at 80 °C using [*p*-DABCO]Cl as the catalyst. As can be seen in Fig. 9, the GLC yield increased rapidly with the reaction time up to 120 min and

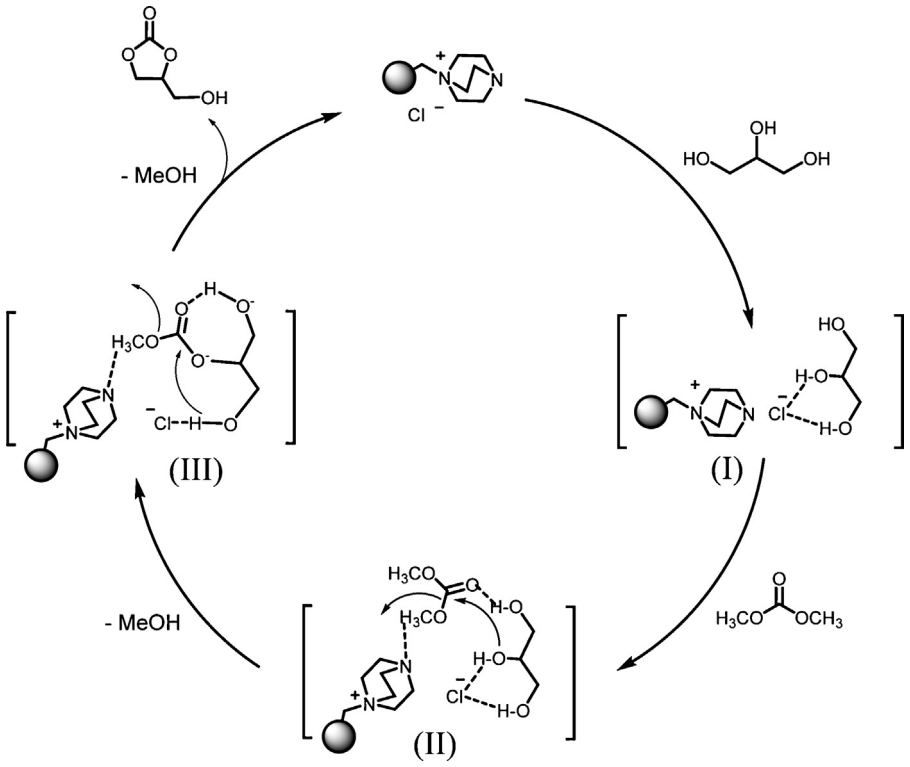

Scheme 3. A plausible mechanism of [*p*-DABCO]Cl-catalyzed transesterification of DMC with glycerol.

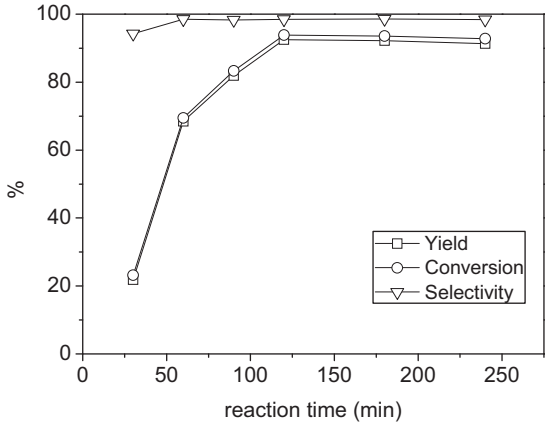

Fig. 9. Effect of reaction time on the [*p*-DABCO]Cl-catalyzed transesterification of DMC with glycerol. Glycerol = 10 g, molar ratio of DMC/glycerol = 2, molar ratio of glycerol/DABCO in [*p*-DABCO]Cl = 100, *T* = 80 °C.

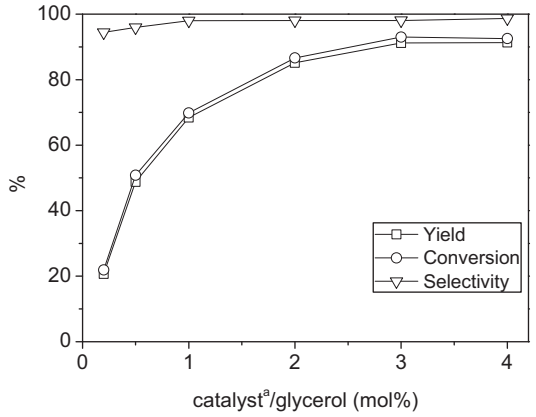

Fig. 11. Effect of catalyst loading on the [*p*-DABCO]Cl-catalyzed transesterification of DMC with glycerol. Glycerol = 10 g, molar ratio of DMC/glycerol = 2, *t* = 1 h, *T* = 80 °C. [a] moles of DABCO in [*p*-DABCO]Cl.

thereafter remained almost constant at 92.5%, implying that equilibrium exists among DMC, glycerol and methanol. By contrast, the selectivity of GLC was maintained at over 98.5% throughout the reaction. Small amounts of side products such as diglycerol tricarbonate were also produced in yields of around 1.0% from the secondary reactions of GLC with DMC or glycerol [4].

The change of GLC yield with the variation of DMC/glycerol molar ratio was also investigated at 80 °C and 60 min. As shown in Fig. 10, the yield of GLC increased from 54.7 to 91.1% with the increase of the molar ratio of DMC/glycerol from 1 to 10. Further increase of the molar ratio to 12 resulted in the decrease of the glycerol conversion and GLC yield, possibly due to the dilution of catalyst concentration. It is noteworthy that the GLC selectivity decreases significantly above the DMC/glycerol molar ratio of 2. It is likely that, at the DMC/glycerol molar ratio above 2, the formation of side products is facilitated by the secondary reactions of GLC with DMC. In fact, the formation of methyl(1,3-dioxolan-2-one-4-yl)methyl carbonate was observed in yield of about 2–5% depending on the reaction condition for all the reactions conducted at the DMC/glycerol molar ratio above 2.

The effect of catalyst loading was also investigated at 80 °C for 1 h. The catalyst loading based on DABCO of [DABCO]Cl was varied in the range from 0.2–4 mol% with respect to the amount of glycerol. As can be seen in Fig. 11, the GLC yield increased with the increase of the molar ratio up to 3 mol%, but remained constant on further increase to 4 mol%. The maximum GLC yield of around 91% is a strong indication that there exist equilibrium between DMC, glycerol, and methanol. Liquid–liquid equilibria for the ternary systems (DMC–methanol–glycerol, DMC–glycerol carbonate–glycerol) and the quaternary system (DMC–methanol–glycerol carbonate–glycerol) have been recently investigated in detail [38]. It is also well known that the reaction of ethylene carbonate with methanol to produce DMC and EG is equilibrium limited [39,40].

The transesterification was conducted in the temperature range of 25–80 °C for 1 h using [*p*-DABCO]Cl as the catalyst. The catalyst loading based on DABCO was fixed at 1 mol% with respect to the amount of glycerol. The yield of GLC increased slowly with the temperature rise up to 70 °C, but increased steeply thereafter (Fig. 12). The rapid increase of GLC yield above 70 °C could be ascribed in part to vaporization loss of co-produced methanol from the reaction system, which would help shift the reaction toward the formation of GLC.

3.5. Catalyst recycle

Facile recovery and reuse of a catalyst are very important in the evaluation of economic feasibility of a process for heterogeneous catalysis. For this reason, we have conducted a catalyst recycle test with the DABCO-immobilized Merrifield resin. For the catalyst recycle test, the resin catalyst was separated by filtration from the product mixture of each transesterification reaction, washed with water, dried under vacuum, and used for the next run. The

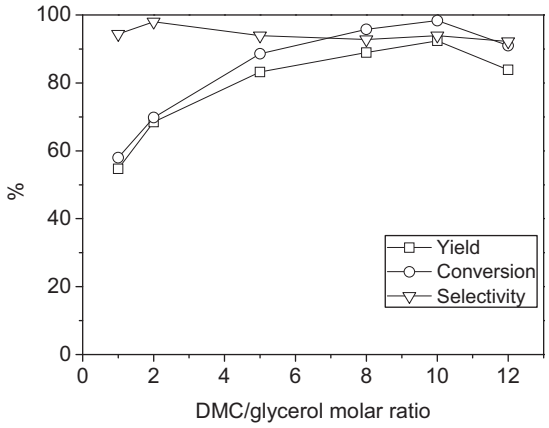

Fig. 10. Effect of DMC/glycerol molar ratio on the [*p*-DABCO]Cl-catalyzed transesterification of DMC with glycerol. Glycerol = 10 g, molar ratio of glycerol/DABCO in [*p*-DABCO]Cl = 100, *t* = 1 h, *T* = 80 °C.

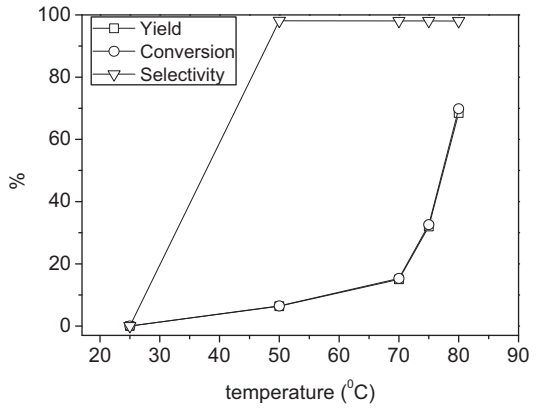

Fig. 12. Effect of temperature on the [*p*-DABCO]Cl-catalyzed transesterification of DMC with glycerol. Glycerol = 10 g, molar ratio of DMC/glycerol = 2, molar ratio of glycerol/DABCO in [*p*-DABCO]Cl = 100, *t* = 1 h.

Table 2
Recycle of [*p*-DABCO]Cl[a]

Run	Yield (%)	Conversion (%)	Selectivity (%)	Elemental analysis (%)		
				C	H	N
Fresh	92.5	94.1	98.2	77.0	7.9	5.3
1	91.9	94.5	97.3	77.0	7.9	5.2
2	91.8	94.0	97.7	–	–	–
3	92.0	94.4	97.5	–	–	–
4	91. 5	93.4	97.9	–	–	–
5	91.4	94.7	96.5	75.9	8.0	5.0

[a] Reaction condition: glycerol = 10 g, molar ratio of glycerol/DABCO in [*p*-DABCO]Cl = 100, DMC/glycerol molar ratio = 2, T = 80 °C, t = 1 h.

elemental analysis results of the fresh [*p*-DABCO]Cl and after 5 uses are listed in Table 2 along with the GLC yields and selectivities. Catalyst deactivation was almost negligible up to 5 cycles on the basis of yield of GLC and the conversion of glycerol. A slight decrease in N and H content after 5 recycles could be ascribed to the possible presence of small amounts of unquaternized DABCO in the fresh catalyst.

4. Conclusions

In summary, we have demonstrated that both DABCO and DABCO-immobilized Merrifield peptide resins, [*p*-DAPCO]Cl can be used as highly active homogeneous and heterogeneous catalysts, respectively, for the transesterification of DMC by glycerol to synthesize GLC. It is noted that the [*p*-DABCO]Cl could be easily recovered and reused at least 5 times. FT-IR studies suggest that there exist a strong hydrogen bonding interaction between a hydroxyl group of glycerol and a nitrogen atom of DABCO, thereby activating glycerol to function as a strong nucleophile to attack on the carbonyl carbon of DMC. In contrast, the activation of glycerol by [*p*-DABCO]Cl seems to proceed through the hydrogen bonding interaction with both Cl^- and the unquaternized nitrogen atom in a cooperative mode. The much higher activity of [*p*-DABCO]Cl than that of [*p*-TMEDA]Cl can be largely attributed to the unique property of [*p*-DABCO]Cl, which is capable of providing favorable environment for the activation of both glycerol and DMC.

Acknowledgements

We acknowledge the financial support by grants from Korea Ministry of Environment as “The Eco-process based technologies” as well as the ‘Creative Allied Project’ grant funded by KRCFS and KIST institutional program (2E24832). This work was also supported by the “Fusion Research Program for Green Technologies (NRF-2012M3C1A1054497)” through the National Research Foundation of Korea (NRF) funded by Ministry of Education, Science and Technology.

Appendix A. Supplementary data

Supplementary data associated with this article can be found, in the online version, at http://dx.doi.org/10.1016/j.apcatb.2014.10.071.

References

[1] Huntsman Corporation, JEFFSOL® Glycerine Carbonate, 2009, http://www.huntsman.com/performance_products/Media/JEFFSOL%20Glycerine%20Carbonate.pdf
[2] D. Randall, R. De Vos, Eur. Patent, EP 419114, 1991.
[3] M. Weuthen, U. Hees, Ger. Patent DE 4335947, 1995.
[4] G. Rokicki, P. Rakoczy, P. Parzuchowski, M. Sobiecki, Green Chem. 7 (2005) 529–539.
[5] L. Ubaghs, N. Fricke, H. Keul, H. Hocker, Macromol. Rapid Commun. 25 (2004) 517–521.
[6] C. Vieville, J.W. Yoo, S. Pelet, Z. Mouloungui, Catal. Lett. 56 (4) (1999) 245–247.
[7] A. Dibenedetto, A. Angelini, M. Aresta, J. Ethiraj, C. Fragale, F. Nocito, Tetrahedron 67 (2011) 1308–1313.
[8] M. Aresta, A. Dibennedetto, F. Nocito, C. Pastore, J. Mol. Catal. A: Chem. 257 (2006) 149–153.
[9] J. George, Y. Patel, S. Pillai, P. Munshi, J. Mol. Catal. A: Chem. 304 (2009) 1–7.
[10] M. Aresta, A. Dibenedetto, F. Nocito, C. Ferragina, J. Catal. 268 (2009) 106–114.
[11] J. Park, J.S. Choi, S.K. Woo, S.D. Lee, M. Cheong, H.S. Kim, H. Lee, Appl. Catal. A 433–434 (2012) 35–40.
[12] M.J. Climent, A. Corma, P.D. Frutos, S. Iborra, M. Noy, A. Veltry, P. Concepcion, J. Catal. 269 (2010) 140–149.
[13] J.R. Ochoa-Gomez, O. Gomez-Jimenez-Aberasturi, B. Maestro-Madurga, A. Pesquera- Rodriguez, C. Ramirez-Lopez, L. Lorenzo-Ibarreta, J. Torrecilla-Soria, M.C. Villaran-Velasco, Appl. Catal. A 366 (2009) 315–324.
[14] F.S.H. Simanjuntak, T.K. Kim, S.D. Lee, B.S. Ahn, H.S. Kim, H. Lee, Appl. Catal. A 401 (2011) 220–225.
[15] J. Li, T. Wang, React. Kinet. Mech. Catal. 102 (2011) 113–126.
[16] J.R. Ochoa-Gómez, O. Gómez-Jiménez-Aberasturi, C. Ramírez-López, B. Maestro-Madurga, Green Chem. 14 (2012) 3368–3376.
[17] M.K. Munshi, S.M. Gade, M.V. Mane, D. Mishra, S. Pal, K. Vanka, V.H. Rane, A.A. Kelkar, J. Mol. Catal. A 391 (2014) 144–149.
[18] M.K. Munshi, S.M. Gade, V.H. Ranea, A.A. Kelkar, RSC Adv. 4 (2014) 32127–32133.
[19] A. Takagaki, K. Iwatani, S. Nishimura, K. Ebitani, Green Chem. 12 (2010) 578–581.
[20] P. Liu, M. Derchib, E.J.M. Hensen, Appl. Catal. A 467 (2013) 124–131.
[21] P. Liu, M. Derchib, E.J.M. Hensen, Appl. Catal. B 144 (2014) 135–143.
[22] F.S.H. Simanjuntak, V.T. Tanda, C.S. Kim, B.S. Ahn, Y.J. Kim, H. Lee, Chem. Eng. Sci. 94 (2013) 265–270.
[23] M. Malyaadri, K. Jagadeeswaraiah, P.S. Sai Prasad, N. Lingaiah, Appl. Catal. A 401 (2011) 153–157.
[24] M.S. Khayoon, B.H. Hameed, Appl. Catal. A 466 (2013) 272–281.
[25] M.J. Frisch, et al., Gaussian 03, Revision C. 02, Gaussian Inc, Wallingford, CT, USA, 2004.
[26] Y.-J. Shi, G. Humphrey, P.E. Maligres, R.A. Reamer, J.M. Williams, Adv. Synth. Catal. 348 (2006) 309–312.
[27] R.N. Ram, V.K. Soni, D.K. Gupta, Tetrahedron 68 (2012) 9068–9075.
[28] O. Nuyken, G. Maier, A. Gross, H. Fischer, Macromol. Chem. Phys. 197 (1997) 83–95.
[29] M.P. Marzocchi, G. Sbrana, G. Zerbi, J. Am. Chem. Soc. 87 (1965) 1429–1432.
[30] Z. Wang, J. Yan, X. Zhang, L. Wang, Synthesis 22 (2009) 3744–3750.
[31] D-Z. Xu, S. Shia, Y. Wang, RSC Adv. 3 (2013) 23075–23079.
[32] A. Hasaninejad, M. Shekouhy, N. Golzar, A. Zare, M.M. Doroodmand, Appl. Catal. A: Gen. 402 (2011) 11–22.
[33] A. Albert, E.P. Serjeant, The Determination of Ionization Constants A Laboratory Manual, third ed., Chapman and Hall, New York, 1984.
[34] V. Lapinte, V. Montembault, A. Houdayer, L. Fontaine, J. Mol. Catal. A: Chem. 276 (2007) 219–225.
[35] R. Lungwitz, S. Spange, New J. Chem. 32 (2008) 392–394.
[36] M.A. Ab Rani, A. Brant, L. Crowhurst, A. Dolan, M. Lui, N.H. Hassan, J.P. Hallett, P.A. Hunt, H. Niedermeyer, J.M. Perez-Arlandis, M. Schrems, T. Welton, R. Wildinga, Phys. Chem. Chem. Phys. 13 (2011) 16831–16840.
[37] P.A. Hunt, B. Kirchner, T. Welton, Chem. Eur. J. 12 (2006) 6762–6775.
[38] J. Esteban, M. Ladero, L. Molinero, F. García-Ochoa, Chem. Eng. Res. Des. (2014), http://dx.doi.org/10.1016/j.cherd.2014.05.026.
[39] M.A. Pacheco, C.L. Marshall, Energ. Fuel. 11 (1997) 2–29.
[40] J.F. Knifton, R.G. Duranleau, J. Mol. Catal. 67 (1991) 389–399.